JOC Article

CASPT2 Study of the Decomposition of Nitrosomethane and Its Tautomerization Reactions in the Ground and Low-Lying Excited States

Juan F. Arenas, Juan C. Otero, Daniel Peláez, and Juan Soto*

Department of Physical Chemistry, Faculty of Sciences, University of Málaga, E-29071-Málaga, Spain

soto@uma.es

Received September 9, 2005

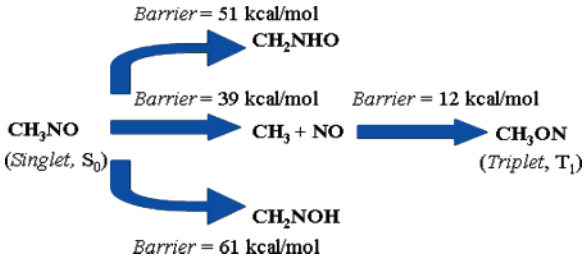

The dissociation reaction of nitrosomethane into methyl and nitric oxide and the tautomerization reactions to formaldehyde oxime, nitrone, and methoxy nitrene have been studied with the second-order multiconfigurational perturbation theory (CASPT2) by the computation of numerical energy gradients. The prevailing reactions in both the ground and the excited states are dissociations. The structures of the ground and excited states are compared with the corresponding complete active space SCF (CAS-SCF) geometries. It is found that changes in the individual bond lengths are rather large (0.01−0.02 Å), while the character and energetics of the CASPT2 optimizations remain similar to the CAS-SCF values.

Introduction

Nitroso compounds are of relevant importance as a result of their broad range of applications, such as synthetic reagents, spin trapping compounds, or high-energy materials.[1] Nitrosoalkanes are biochemically important as well, for example, they form stable complexes with Fe^{III} heme enzymes after the biodegradation of aliphatic nitroalkanes, a process which seems to be involved in the carcinogenic activity of the nitro compounds.[2]

The monomers of nitrosomethane (CH_3NO) are blue in color in solvents of a low dielectric constant, while in aqueous solutions, they are colorless. The solid is white and is characterized as a dimer that results from the N−N interaction to give diazene dioxides: both cis and trans dimers $(CH_3NO)_2$ of nitrosomethane are known.[1,3] Heating *cis*-$(CH_3NO)_2$ up to ∼80 °C gives formaldehyde oxime (CH_2NOH), while at ∼95 °C, monomeric CH_3NO is the major product.[4] Heating *trans*-$(CH_3NO)_2$ at ∼28 °C gives the trans dimer instead of the monomeric compound.[4] Photochemical reactions of nitrosomethane in the gas phase are known after excitation in the visible band around 600−700 nm. The prevailing reaction of the photolysis is the C−N bond breaking to yield CH_3 plus NO ($X^2\Pi$).[5] The tautomerization of nitrosomethane to formaldehyde oxime occurs readily in aqueous solutions when hydroxylic groups are present, which suggests effective acid/base catalysis by protic solvents.[1]

Our interest in nitroso compounds arises from the fact that they are products of the photolysis of nitro derivatives.[6] The aim of this work is to study the thermal and photochemical reactions of nitrosomethane leading to (i) dissociation into

(1) Long, J. A.; Harris, N. J.; Lammertsma, K. *J. Org. Chem.* **2001**, *66*, 6762 and references therein.

(2) Bouros, J.; Bayachou, M. *Inorg. Chem.* **2004**, *43*, 3847 and references therein.

(3) (a) Meerssche, M. v.; Germain, G. *Bull. Soc. Chim. Belg.* **1959**, *68*, 244. (b) Germain, G.; Piret, P.; Meerssche, M. v. *Acta Crystallogr.* **1963**, *16*, 109.

(4) Frost, D. C.; Lau, W. M.; McDowell, C. A.; Westwood, N. P. C. *J. Phys. Chem.* **1982**, *86*, 3577.

(5) (a) McCoustra, M. R. S.; Pfab, J. *Spectrochim. Acta, Part A* **1990**, *46*, 937. (b) Toniolo, A.; Persico, M. *J. Chem. Phys.* **2001**, *115*, 1817.

(6) (a) Arenas, J. F.; Otero, J. C.; Peláez, D.; Soto, J. *J. Chem. Phys.* **2005**, *122*, 084324. (b) Arenas, J. F.; Otero, J. C.; Peláez, D.; Soto, J. *J. Phys. Chem. A* **2005**, *109*, 7172. (c) Arenas, J. F.; Otero, J. C.; Peláez, D.; Soto, J. *J. Chem. Phys.* **2003**, *119*, 7814. (d) Arenas, J. F.; Centeno, S. P.; López-Tocón, I.; Peláez, D.; Soto, J. *J. Mol. Struc.−THEOCHEM* **2003**, *630*, 17. (e) Arenas, J. F.; Otero, J. C.; Peláez, D.; Soto, J.; Serrano-Andrés, L. *J. Chem. Phys.* **2004**, *121*, 4127.

10.1021/jo051897r CCC: $33.50
Published on Web 01/11/2006

methyl (CH_3) and nitric oxide (NO), (ii) tautomerization to oxime (CH_2N-OH), (iii) tautomerization to nitrone (CH_2NH-O), and (iv) isomerization to methoxy nitrene (CH_3ON).

Methods of Calculation

Generally contracted basis sets of the atomic natural orbital (ANO) type obtained from C,N,O(14s9p4d3f)/H(8s4p3d) primitive sets,[7] the so-called ANO-L basis sets, with the C,N[4s3p2d1f]/H[3s2p1d] contraction schemes were used in all of the geometry optimizations of the relevant species involved in the photolysis of nitromethane, hereafter called ANO-L basis sets (I). These optimizations were performed following two strategies: (i) optimization at the complete active space SCF (CAS-SCF)[8] level of theory by the computation of analytical energy gradients and (ii) optimizations with the second-order multiconfigurational perturbation theory (CASPT2)[9] by the computation of numerical energy gradients. Both methods were applied as implemented in the MOLCAS 6.2 program.[10] In the CASPT2 calculation, the 1s electrons of the carbon, oxygen, and nitrogen atoms, as determined in the SCF calculations, were kept frozen. On the other hand, the localization of the crossing points (conical intersections and intersystem crossings) were done with the algorithm implemented in the Gaussian program[11a] and with the cc-p valence double zeta basis set.[12] The gradient difference and nonadiabatic coupling vectors are computed using state-average orbitals in the manner suggested by Yarkony.[11b,c] Although this procedure requires the computation of the Hessian matrix at each iteration, the contributions that arise from the derivatives of the orbital rotations have been neglected.[11b]

The stationary points (minima and saddle points) were characterized by their CAS-SCF analytic harmonic vibrational frequencies, computed by diagonalizing the mass-weighted Cartesian force constant matrix.

Across this manuscript, figures representing energy profiles are linear interpolations. These curves are obtained via the interpolation between initial and final stationary geometries, the latter can correspond to dissociation products. Therefore, in fact, the two-dimensional plots are not true reaction paths but cuts of the multidimensional potential energy surface along an arbitrary direction. However, they provide good initial guesses for the optimizations of crossing points and transition states. On the other hand, if no barrier is found along a dissociation interpolation, then it will not exist along the true energy path.

TABLE 1. MS-CASPT2 Vertical Excitation Energies and Oscillator Strengths for the Electronic States of Nitrosomethane[a,b]

state	configuration	weight[c]	ΔE (eV)	osc. str.
ground state		89		
2A′	$(n_\sigma)^0(\pi^*_{NO})^2$	88	4.96	7.65×10^{-5}
			(4.75)[c]	(8.16×10^{-5})
3A′	$(n_\sigma)^1(3p)^1$	61	6.54	8.64×10^{-3}
	$(n_\sigma)^1(3s)^1$	29		
4A′	$(n_\sigma)^1(3p)^1$	29	7.20	3.75×10^{-2}
	$(n_\sigma)^1(3s)^1$	61		
5A′	$(\pi_{NO})^1(\pi^*_{NO})^1$	87	9.44	3.08×10^{-5}
1A″	$(n_\sigma)^1(\pi^*_{NO})^1$	89	1.76	5.12×10^{-4}
			(1.66)	(5.92×10^{-3})
2A″	$(\sigma_{NO})^1(\pi^*_{NO})^1$	67	6.29	1.51×10^{-3}
	$(n_\sigma)^1(\pi_{NO})^1(\pi^*_{NO})^2$	26	(6.09)	(6.00×10^{-3})
3A″	$(n_\sigma)^1(3p)^1$	87	7.37	1.77×10^{-2}

[a] ANO-L basis sets (II) and CAS-SCF (12e,o) reference wave function. The imaginary level shift is equal to 0.1. [b] Geometry optimized at the CASPT2 level with the ANO-L basis sets (I). [c] Weight of the main electronic configuration in %. [d] The values in parentheses were obtained with the ANO-L basis sets (I).

Results and Discussion

Electronic Structure of Nitrosomethane and Vertical Excitation Energies. The electronic configuration of nitrosomethane at the ground-state geometry can be described as

$$a': (1s_O)(1s_N)(1s_C)(2s_O)(\sigma CH_3)(2s_N)(\sigma NO)(\sigma CN)(\sigma CH_3)(n_\sigma NO)$$

$$a'': (\pi NO)(\sigma CH_3)$$

Nitrosomethane has several electronic states of Rydberg character localized at rather low energy[13] that could be involved in the photochemistry of this compound. Consequently, an exploring of the excited-state potential energy surfaces becomes demanding. To take into account the electronic transitions to Rydberg states, the C;N,O(14s9p4d)/H(8s4p3d) primitive sets of the ANO-L basis, contracted with the C;N,O(3s2p1d)/H(2s1p) scheme, have been supplemented with a 1s3p set of diffuse functions (contracted from eight primitives for each angular momentum type),[14] which were built following the procedure described by Roos and co-workers.[15] Hereafter, it is called ANO-L basis sets (II). Table 1 collects the vertical excitation energies calculated with the extended multistate CASPT2 (MS-CASPT2) approach[16] whose CAS-SCF reference function is built from an active space of 12 electrons distributed in 12 orbitals. The active space comprises the following valence orbitals: ($2s_O$), ($2s_N$), (σNO), (σCN), (n_σNO), (πNO), (σ^*NO), (σ^*CN), and (π^*NO), plus one 3s Rydberg, two 3p Rydberg orbitals of a′ symmetry, and one 3p Rydberg orbital of a″ symmetry. Valence orbitals in the active space are sketched in Scheme 1 and represented in Figure S1 (Supporting Information). To minimize the contamination of the perturbed wave

(7) Widmark, P.-O.; Malmqvist, P.-Å.; Roos, B. O. *Theor. Chim. Acta* **1990**, *77*, 291.
(8) Roos, B. O. In *Advances in Chemical Physics; Ab Initio Methods in Quantum Chemistry II*; Lawley, K. P., Ed.; John Wiley & Sons: Chichester, England, 1987; Chapter 69, p 399.
(9) (a) Anderson, K.; Malmqvist, P.-Å.; Roos, B. O.; Sadlej, A. J.; Wolinski, K. *J Phys. Chem.* **1990**, *94*, 5483. (b) Anderson, K.; Malmqvist, P.-Å.; Roos, B. O. *J. Chem. Phys.* **1992**, *96*, 1218.
(10) Andersson, K. et al. *MOLCAS*, version 6.2; Lund University: Sweden, 2005.
(11) (a) Frisch, M. J.; Trucks, G. W.; Schlegel, H. B.; Scuseria, G. E.; Robb, M. A.; Cheeseman, J. R.; Montgomery, J. A., Jr.; Vreven, T.; Kudin, K. N.; Burant, J. C.; Millam, J. M.; Iyengar, S. S.; Tomasi, J.; Barone, V.; Mennucci, B.; Cossi, M.; Scalmani, G.; Rega, N.; Petersson, G. A.; Nakatsuji, H.; Hada, M.; Ehara, M.; Toyota, K.; Fukuda, R.; Hasegawa, J.; Ishida, M.; Nakajima, T.; Honda, Y.; Kitao, O.; Nakai, H.; Klene, M.; Li, X.; Knox, J. E.; Hratchian, H. P.; Cross, J. B.; Bakken, V.; Adamo, C.; Jaramillo, J.; Gomperts, R.; Stratmann, R. E.; Yazyev, O.; Austin, A. J.; Cammi, R.; Pomelli, C.; Ochterski, J. W.; Ayala, P. Y.; Morokuma, K.; Voth, G. A.; Salvador, P.; Dannenberg, J. J.; Zakrzewski, V. G.; Dapprich, S.; Daniels, A. D.; Strain, M. C.; Farkas, O.; Malick, D. K.; Rabuck, A. D.; Raghavachari, K.; Foresman, J. B.; Ortiz, J. V.; Cui, Q.; Baboul, A. G.; Clifford, S.; Cioslowski, J.; Stefanov, B. B.; Liu, G.; Liashenko, A.; Piskorz, P.; Komaromi, I.; Martin, R. L.; Fox, D. J.; Keith, T.; Al-Laham, M. A.; Peng, C. Y.; Nanayakkara, A.; Challacombe, M.; Gill, P. M. W.; Johnson, B.; Chen, W.; Wong, M. W.; Gonzalez, C.; Pople, J. A. *Gaussian 03*, revision B.04; Gaussian, Inc.: Wallingford, CT, 2004. (b) Bearpark, M. J.; Robb, M. A.; Schlegel, H. B. *Chem. Phys. Lett.* **1994**, *223*, 269. (c) Yarkony, D. R. *J. Chem. Phys.* **1990**, *92*, 2457.
(12) Dunning, T. H., Jr. *J. Chem. Phys.* **1989**, *90*, 1007.
(13) Lacombe, S.; Loudet, M.; Dargelos, A.; Camou, J. M. *Chem. Phys.* **2001**, *258*, 1.
(14) Kaufmann, K.; Baumeister, W.; Jungen, M. *J. Phys. B: At. Mol. Opt. Phys.* **1989**, *22*, 2223.
(15) Roos, B. O.; Fülscher, M. P.; Malmqvist, P.-Å.; Merchán, M.; Serrano-Andrés, L. In *Quantum Mechanical Electronic Structure Calculations with Chemical Accuracy*; Langhoff, S. R., Ed.; Kluver Academic Publisher: Dordrecht, The Netherlands, 1995; p 357.
(16) Finley, J.; Malmqvist, P.-Å.; Roos, B. O.; Serrano-Andrés, L. *Chem. Phys. Lett.* **1998**, *288*, 299.

SCHEME 1

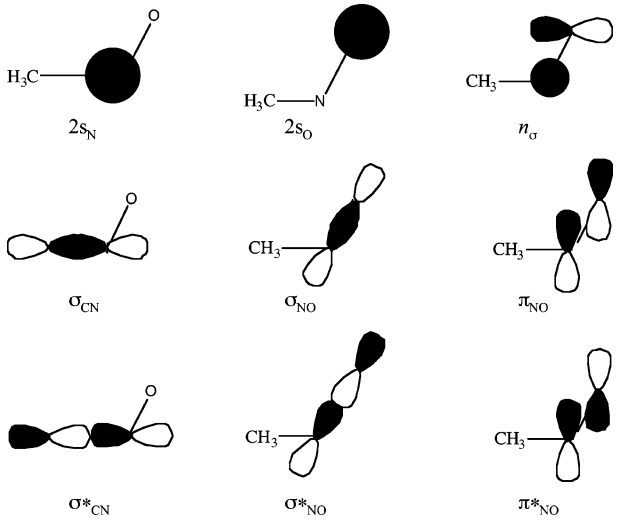

TABLE 2. CASPT2 Energies of the Critical Points of the Dissociation of Nitrosomethane into Methyl and Nitric Oxide on the Singlet and Triplet Surfaces[a]

geometry	configuration	ΔE (kcal/mol)
M1, Figure 1a, 1A′	ground state	0.0
M2, Figure 1b, 1A″	$(n_\sigma)^1(\pi^*_{NO})^1$	34.4
Ts1, Figure 1c, 1A″	$(n_\sigma)^1(\pi^*_{NO})^1$	47.4
M3, Figure 1d, 2A′	$(n_\sigma)^0(\pi^*_{NO})^2$	72.0
M4, Figure 1e, 2A″	$(\sigma_{NO})^1(\pi^*_{NO})^1$	110.0
M5, Figure 1f, 1^3A″	$(n_\sigma)^1(\pi^*_{NO})^1$	14.4
M6, Figure 1g, 1^3A′	$(\pi_{NO})^1(\pi^*_{NO})^1$	80.6
Ts2, Figure 1h, 1^3A″	$(n_\sigma)^1(\pi^*_{NO})^1$	41.6
Isc1, Figure 1i, 1^3A″/1A′	T_1/S_0	17.8
Isc1b, Figure 1j, 1^1A″/1^3A″	S_1/T_1	82.0
Ci0, Figure 1k, 1^1A″/1A′	S_1/S_0	49.0

[a] ANO-L basis sets (I) and CAS-SCF (12e, 9o) reference wave function.

function by intruder states, the technique of the imaginary level shift[17] has been introduced in all the computed energies. The oscillator strengths, given in Table 1 as well, were computed according to the CAS state interaction procedure[18] in conjunction with the perturbatively modified CAS reference functions obtained as linear combinations of all the states involved in the MS-CASPT2 calculation.

Our results agree with the data previously reported by Lacombe et al.[13] and with the only experimentally available value, that is, the A′ → A″ vertical excitation whose Franck−Condon forbidden origin was estimated at 1.79 eV.[19] The computed value in this work for the vertical excitation energy is 1.76 eV (40.6 kcal/mol), which compares with the value reported by Toniolo and Persico[5b] (T_v = 39.7 kcal/mol). To our concern, it is important to note that the four lowest singlets are valence states.

Dissociation of Nitrosomethane into Methyl and Nitric Oxide. $CH_3NO \rightarrow CH_3 + NO$. In this section, the main features of the singlet and triplet surfaces related to the production of nitric oxide will be stressed. The energetic data for all the critical points of this decomposition reaction are collected in Table 2, the geometrical parameters are collected in Table S1 (Supporting Information), and the optimized structures for such points are displayed in Figure 1. Geometrical and energetic data are calculated both at the CASPT2 and CAS-SCF levels by using a CAS-SCF reference wave function, which includes 12 electrons distributed in nine orbitals (Scheme 1 and Figure S1 in Supporting Information). In labeling the critical points,

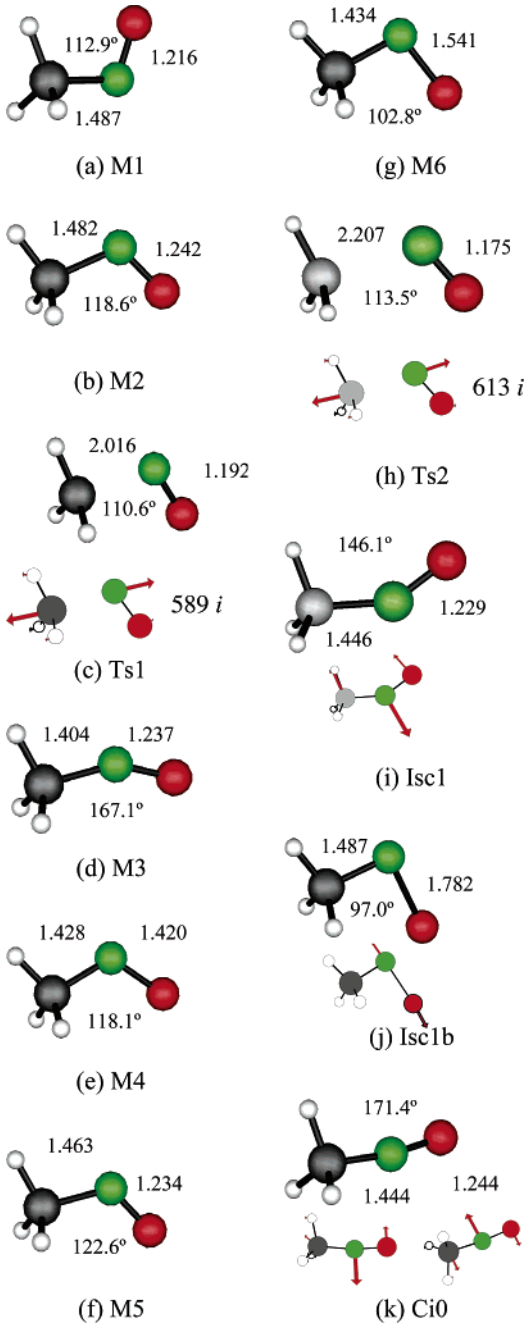

FIGURE 1. CASPT2 geometries for the decomposition of nitrosomethane into CH_3 and NO in the ground state and the three low-lying excited states. The arrows in the smaller figures correspond to the (i) imaginary mode (stationary points), (ii) gradient difference vector (intersystem crossings), or (iii) nonadiabatic coupling (right) and gradient difference (left) vectors (for conical intersections). (a) S_0 (1A′) minimum; (b) S_1 (1A″) minimum; (c) S_1 transition state; (d) S_2 (2A′) minimum; (e) S_3 (2A″) minimum; (f) T_1 (13A″) minimum; (g) T_2 (1^3A′) minimum; (h) T_1 (1^3A″) transition state; (i) CAS-SCF T_1/S_0 intersystem crossing; (j) CAS-SCF S_1/T_1 intersystem crossing; (k) CAS-SCF S_1/S_0 conical intersection. Structures are represented with the MacMolplt program.[32]

(17) Forsberg, N.; Malmqvist, P.-Å. *Chem. Phys. Lett.* **1997**, *274*, 196.
(18) (a) Malmqvist, P.-Å. *Int. J. Quantum Chem.* **1986**, *30*, 470. (b) Malmqvist, P.-Å.; Roos, B. O. *Chem. Phys. Lett.* **1989**, *155*, 189.
(19) Ernsting, N. P.; Pfab, J.; Römelt, J. *J. Chem. Soc., Faraday Trans. 2* **1978**, *74*, 2286.

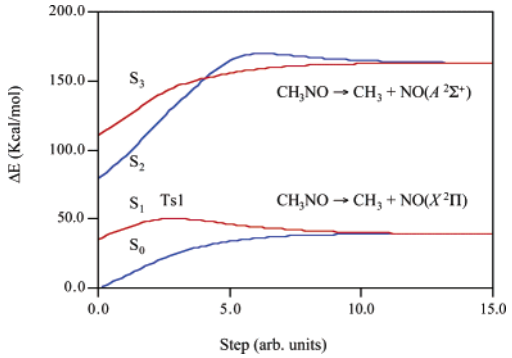

FIGURE 2. Singlet MS-CASPT2/ANO-L linear interpolations (C_s symmetry) for the dissociation of nitrosomethane in the ground state and the three low-lying excited states. The geometry of the initial points corresponds to the minima of nitrosomethane in the corresponding state.

minima, transition states, conical intersections, intersystem crossings, and nonstationary structures are denoted by M*n*, Ts*n*, Ci*n*, Isc*n*, and Ns*n*, where *n* is a number. Roughly, our CAS-SCF geometrical parameters agree with those given by Toniolo and Persico[5b] and Dolgov et al.[20] for the S_0, S_1, and T_1 states of nitrosomethane. The main differences between these data can be attributed to different active spaces used in each case.

The energy profiles of the linear interpolations for the dissociation of nitrosomethane into the methyl radical and the nitric oxide in four singlet valence states are represented in Figure 2. The minimum of nitrosomethane on the S_0 surface has an eclipsed conformation (M1, Figure 1a). There is no exit barrier for the dissociation of the ground state, in agreement with Zhang et al.[21] The bond dissociation energy for such a reaction amounts to 39 kcal/mol, which compares with the value reported by Toniolo and Persico[5b] (38.3 kcal/mol) and with the experimental data presented by Wollf and Wagner[22] (39 kcal/mol) and Jodkowski et al.[23] (40.3 kcal/mol). In contrast, S_1 nitrosomethane has a staggered conformation (M2, Figure 1b), as was demonstrated by Ernsting et al.[19] in an experimental work. This state has an exit barrier for C−N bond breaking with an energy height of ∼13 kcal/mol above M2 (Ts1, Figure 1c). The computed value for the bond dissociation energy amounts to 4.5 kcal/mol, which differs slightly from the value of −0.3 kcal/mol reported in ref 5b. Both S_0 and S_1 states yield nitric oxide in their degenerate ground state. Alternatively, the S_2 and S_3 states decompose adiabatically into excited nitric oxide. Their respective dissociation curves are represented in Figure 2 as well, where the energy barriers are seen to be appreciably greater than those of the two lowest states.

Nitrosomethane has a triplet state ($1^3A''$) with a staggered conformation (M5, Figure 1f) localized at rather low energy (14.4 kcal/mol) above M1. Another triplet minimum of A′ symmetry exists (M6, Figure 1g), but this is 80.6 kcal/mol above M1 and it does not seem to be chemically important in our discussion. Figure 3a illustrates the dissociation curves of the first triplet ($1^3A''$). M5 must surmount an energy barrier of 27.3 kcal/mol above M5 to reach the transition state leading to dissociation (Ts2, Figure 1h). Its bond dissociation energy amounts to ∼25 kcal/mol, which is slightly higher than a previously reported value (∼19 kcal/mol).[5b] In addition, we were able to optimize the lowest energy point in the seam of crossing between the S_0 and T_1 surfaces (Isc1, Figure 1i), which is only 17.8 kcal/mol above M1. The energy profile of the S_0/T_1 crossing is given in Figure 3b along with the magnitude of the spin−orbit coupling estimated as[24]

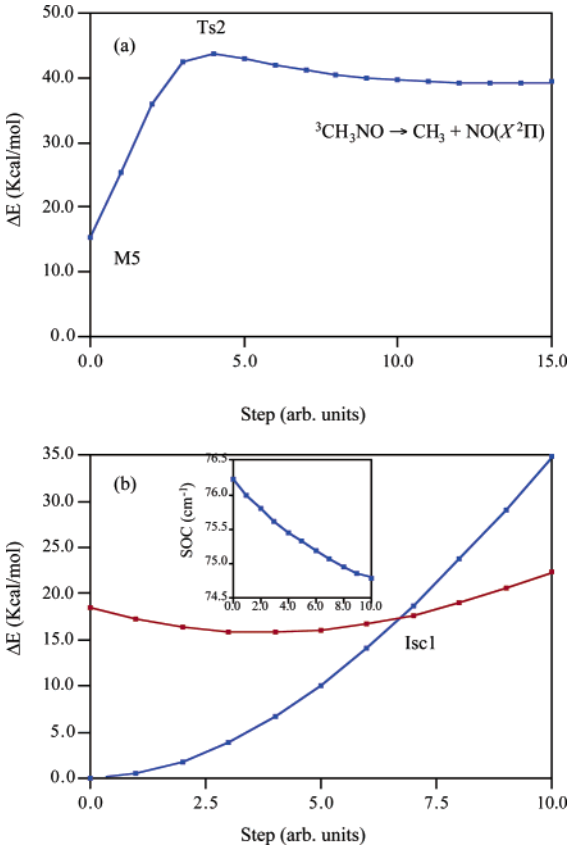

FIGURE 3. (a) CASPT2/ANO-L linear interpolation (C_s symmetry) for the dissociation of nitrosomethane in the lowest triplet state. (b) Energy profile of the S_0 and T_1 surfaces (CASPT2) of the linear interpolation between the minimum of nitrosomethane and the Isc1 (CAS-SCF). Spin−orbit coupling is represented in the inset.

$$SOC_{rms} = \left(\sum_{M_S} |SOC(M_S)|^2\right)^{1/2} \quad (1)$$

The preceding discussion might suggest that a very efficient $S_0 \rightarrow T_1$ intersystem crossing should be present in the dissociation dynamics of nitrosomethane, which would lead to a dissociation in two steps: (i) $S_0 \rightarrow T_1$ intersystem crossing and (ii) C−N bond breaking in the first triplet state. However, we think that this process is not likely to occur. In fact, some exploratory dynamical calculations performed at the MP2 level on the S_0 surface have been unsuccessful in sampling the crossing region.

To finish this section, we will address an issue uncovered by one of the referees. Provided that we are using a quite good level of theory, the computed barrier for dissociation on the first excited state (47.4 kcal/mol) seems to be rather high when

(20) (a) Dolgov, E. K.; Bataev, V. A.; Godunov, I. A. *Int. J. Quantum Chem.* **2004**, *96*, 193. (b) Dolgov, E. K.; Bataev, V. A.; Pupyshev, V. I.; Godunov, I. A. *Int. J. Quantum Chem.* **2004**, *96*, 589.

(21) Zhang, J.-X.; Liu, J.-Y.; Li, Z.-S.; Sun, C.-C. *J. Comput. Chem.* **2005**, *26*, 807.

(22) Wollf, T.; Wagner, H. G. *Ber. Bunsen-Ges. Phys. Chem.* **1998**, *92*, 678.

(23) Jodkowski, J. T.; Ratajczak, E.; Sillesen, A.; Pagsberg, P. *Chem. Phys. Lett.* **1993**, *203*, 490.

(24) Furlani, T. R.; King, H. F. *J. Chem. Phys.* **1985**, *82*, 5577.

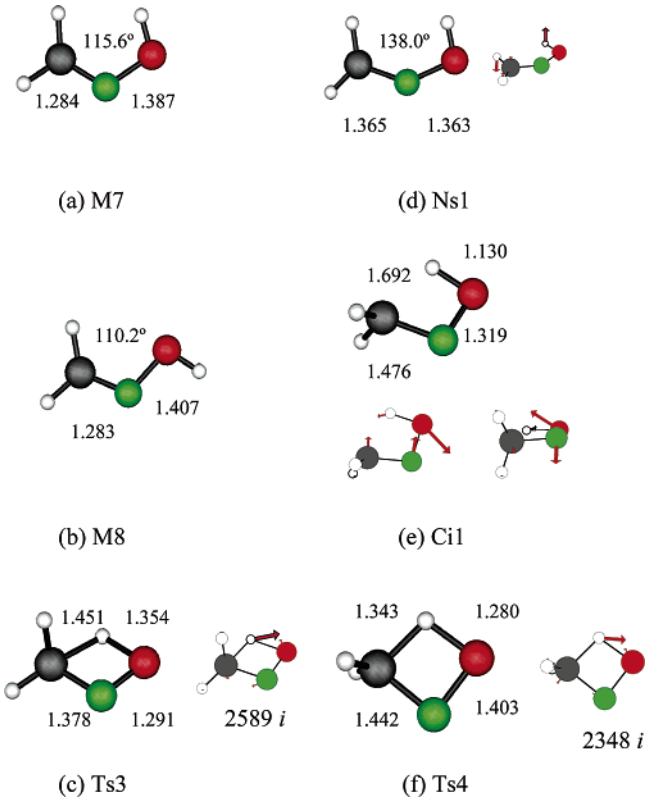

FIGURE 4. Relevant geometries for the nitroso-oxime isomerization on the S_0 and S_1 surfaces at the CASPT2 level. The arrows in the smaller structures correspond to (i) imaginary modes (for stationary points) or (ii) nonadiabatic coupling (right) and gradient difference (left) vectors (for conical intersections). (a) S_0 *s-cis*-formaldehyde oxime (C_s); (b) S_0 *s-trans*-formaldehyde oxime (C_s); (c) S_0 transition state for the nitroso-oxime isomerization (C_1); (d) S_1 constrained optimization of *s-cis*-formaldehyde oxime (C_s); (e) S_1/S_0 conical intersection; (f) S_1 transition state for the nitroso-oxime isomerization (C_s). Structures are represented with the MacMolplt program.[32]

compared with experimental values. As suggested by the reviewer, we have searched for a S_1/T_1 intersystem crossing and we have found such a critical point (Isc1b, Figure 1j) located at too high an energy, 82.0 kcal/mol above M1; furthermore, Isc1b shows a very small magnitude of the spin−orbit coupling constant (1−3 cm^{-1}). Consequently, this deactivation mechanism is seen as rather improbable. In addition, we were able to find a low-energy conical intersection (Ci0, Figure 1k), which is located at 49 kcal/mol above M1. Therefore, this path would be a competitive deactivation channel that would lead to dissociation on the S_0 state. One of the reasons why the computed energies are still high for both deactivation mechanisms (predissociation and internal conversion) might be that the S_0-S_1 transition arises from a hot band of nitrosomethane, as it was first proposed by Dixon and Kroto.[25] Obviously, another reason is the intrinsic limitations of the CASPT2 method.

Tautomerization of Nitrosomethane to Formaldehyde Oxime. $CH_3NO \rightarrow CH_2N-OH$. Figure 4 displays the critical structures found at the CASPT2 level in the isomerization reaction of nitrosomethane to formaldehyde oxime in the ground and first excited states by using a CAS-SCF reference wave function that includes 14 electrons distributed in 11 orbitals, that is, the orbitals involved in the dissociation mechanism, plus the σCH and σ*CH orbitals of the migrating hydrogen. The energies of all the geometries discussed in this section are summarized in Table 3.

TABLE 3. CASPT2 Energies of the Critical Points for the $CH_3NO \rightarrow CH_2NOH$ Tautomerization[a]

geometry	configuration	ΔE (kcal/mol)
M1, Figure 1a, 1A′	ground state	0.0
M7, Figure 4a, 1A′	ground state	−8.4
M8, Figure 4b, 1A′	ground state	−13.6
Ts3, Figure 4c	ground state	61.0
Ns1, Figure 4d, 1A″	$(n_\sigma)^1(\pi^*_{CN})^1$	112.3
Ci1, Figure 4e, 1A″/1A′	S_1/S_0	79.3
Ts4, Figure 4f, 1A″	$(n_\sigma)^1(\pi^*_{NO})^1$	77.9

[a] ANO-L basis sets (I) and CAS-SCF (14e, 11o) reference wave function.

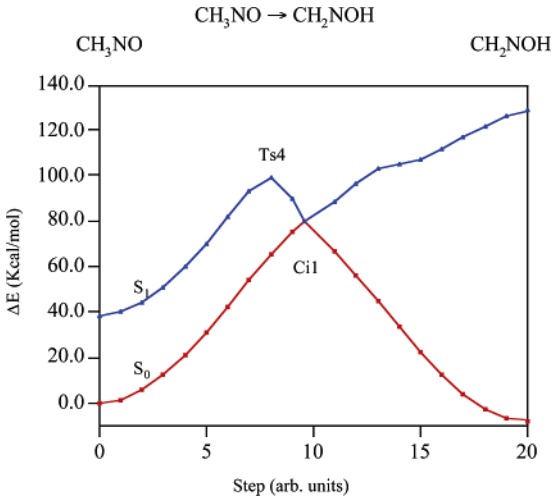

FIGURE 5. Energy profile of the linear interpolation of the $CH_3NO \rightarrow CH_2NOH$ tautomerization, showing the path through the Ci1 conical intersection.

The relevant points on the S_0 surface of this reaction are: (i) nitrosomethane (M1 minimum, Figure 1a), (ii) *s-cis*-formaldehyde oxime (M7 minimum, Figure 4a), (iii) *s-trans*-formaldehyde oxime (M8 minimum, Figure 4b), and (iv) the transition state leading to the isomerization of nitrosomethane to *s-cis*-formaldehyde oxime (Ts3, Figure 4c). The barrier height for the nitroso to *s-cis*-oxime isomerization amounts to 61.0 kcal/mol. In the S_1 first excited state, nitrosomethane has a minimum with an alternated conformation (M2, Figure 1b); however, formaldehyde oxime does not exhibit any stationary geometry on the S_1 surface. A C_s symmetry constrained optimization of the S_1 oxime yields the structure plotted in Figure 4d (Ns1). The projected Hessian matrix[26] of Ns1 gives the steepest descent mode as that pointing to a conical intersection (Ci1, Figure 4e). The energy profile of the S_0 and S_1 surfaces passing through Ci1 is given in Figure 5. As it is shown in this graphic, it does not seem that the S_1 nitroso-oxime isomerization is a likely process because it has to surmount an energy barrier before decaying to the S_0 state through Ci1. In fact, we were able to optimize the transition state leading from S_1 nitrosomethane to Ci1 (Ts4, Figure 4f); the energy associated with this transition geometry amounts to 78 kcal/mol above M1. On the other hand, the excitation of the formaldehyde oxime into the S_1 state will

(25) Dixon, R. N.; Kroto, H. W. *Proc. R. Soc. London, Ser. A* **1964**, *283*, 423.

(26) Polasek, M.; Turecek, F. *J. Am. Chem. Soc.* **2000**, *122*, 525.

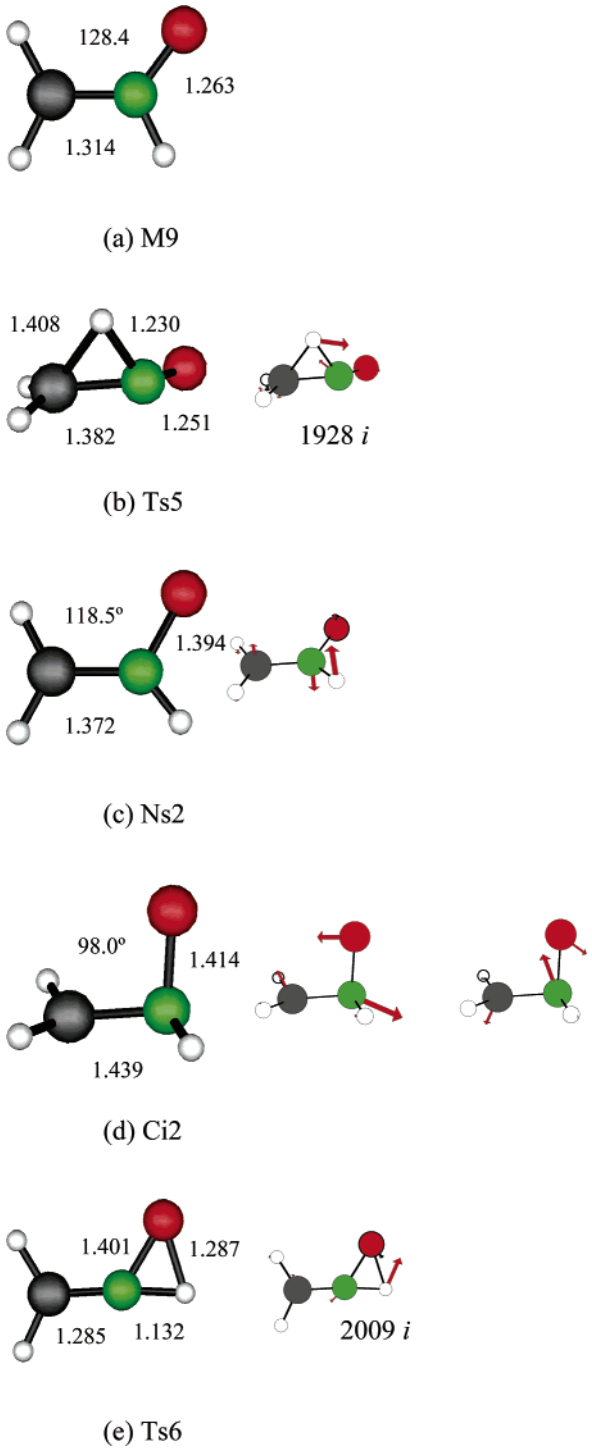

FIGURE 6. Relevant geometries for the isomerization of nitrosomethane to nitrone on the S_0 and S_1 surfaces at the CASPT2 level. The arrows in the smaller structures correspond to the (i) imaginary modes (for stationary points) or (ii) nonadiabatic coupling (right) and gradient difference (left) vectors (for conical intersections). (a) S_0 nitrone (C_s); (b) S_0 transition state for the nitroso-nitrone isomerization (C_1); (c) S_1 constrained optimization of nitrone (C_s); (d) S_1/S_0 conical intersection; (e) S_0 transition state for isomerization of nitrone to *s-trans*-formaldehyde oxime (C_s). Structures are represented with the MacMolplt program.[32]

lead directly to Ci1 via a barrierless path, as shown in Figure 5. The directions of the gradient difference and nonadiabatic coupling vectors of Ci1 suggest that the domains of both the

TABLE 4. CASPT2 Energies of the Critical Points for the $CH_3NO \rightarrow CH_2NHO$ Tautomerization[a]

geometry	configuration	ΔE (kcal/mol)
M1, Figure 1a, 1A′	ground state	0.0
M9, Figure 6a, 1A′	ground state	−3.0
Ts5, Figure 6b, 1A′	ground state	50.9
Ns2, Figure 6c, 1A″	$(n_\sigma)^1(\pi^*_{CN})^1$	82.8
Ci2, Figure 6d, 1A″/1A′	S_1/S_0	60.3
Ts6, Figure 6e, 1A″	$(n_\sigma)^1(\pi^*_{NO})^1$	41.6

[a] ANO-L basis sets (I) and CAS-SCF (14e, 11o) reference wave function.

nitrosomethane and the oxime could be populated after decaying to the S_0 state through this crossing point. The dissociation paths of formaldehyde oxime leading to (i) $^2CH_2N + {}^2OH$ (Figure S2a, Supporting Information) and (ii) $^3CH_2 + {}^3NOH$ (Figure S2b, Supporting Information) yield 64 and 136 kcal/mol, respectively, for the bond dissociation energies.

Tautomerization of Nitrosomethane to Nitrone. $CH_3NO \rightarrow CH_2NH{-}O$. Figure 6 represents the critical structures found at the CASPT2 level in the isomerization reaction of nitrosomethane to nitrone in the ground and first excited states by using a CAS-SCF reference wave function with an active space of 14 electrons distributed in 11 orbitals, that is, the orbitals involved in the dissociation mechanism, plus the σCH and σ*CH orbitals of the migrating hydrogen.

On the S_0 surface of this reaction we have found the minimum of the nitrone (M9, Figure 6a) and the transition state leading to the isomerization of nitrosomethane to nitrone (Ts5, Figure 6b). The barrier height for the nitroso to nitrone isomerization amounts to 50.9 kcal/mol, which compares with the barriers estimated by other authors, 50 kcal/mol at 298 K by Polasek and Turecek[27] with the G2(MP2) method, 47 kcal/mol by Alcami et al.[28] at the B3LYP level, and 51 kcal/mol by Vladimiroff[29] at the B3LYP level. The nitrone does not exhibit any stationary geometry on the S_1 surface. A constrained optimization of the S_1 nitrone in C_s symmetry yields the structure plotted in Figure 6c (Ns2). The projected Hessian matrix of Ns2 gives the steepest descent mode as that pointing to a conical intersection (Ci2, Figure 6d). Direct nitroso-nitrone isomerization in the S_1 state would imply that an energy barrier (upper limit) of approximately 95 kcal/mol was surmounted before the decay to the S_0 state through Ci2; therefore, this process must not be likely. On the other hand, an interpolation line shows that the excitation of the nitrone into the S_1 state will lead directly to Ci2 via a barrierless path. Accordingly, deactivation of the S_1 nitrone via Ci2 would yield the S_0 nitrone again. The isomerization of the nitrone (M9) to *s-trans*-formaldehyde oxime (M8) has been studied as well. The transition state for such a reaction (Ts6, Figure 6e) is 44.6 kcal/mol higher than the S_0 minimum of the nitrone. The dissociation of nitrone into methylene and nitroso hydrogen ($CH_2NHO \rightarrow {}^3CH_2 + {}^1HNO$, Figure S3) has a bond dissociation energy of 105 kcal/mol. The energies of all the geometries discussed in this section are summarized in Table 4.

Isomerization of Nitrosomethane to Methoxy Nitrene. $CH_3NO \rightarrow CH_3ON$. To our knowledge, methoxy nitrene (CH_3ON) has not yet been observed. Its parent molecule

(27) Alcami, M.; Mó, O.; Yáñez, M.; Luna, A.; Morizur, J.-P.; Tortajada, J. *J. Phys. Chem. A* **1998**, *102*, 10120.
(28) Vladimiroff, T. *THEOCHEM* **1997**, *401*, 141.
(29) Arenas, J. F.; Marcos, J. I.; López-Tocón, I.; Otero, J. C.; Soto, J. *J. Chem. Phys.* **2000**, *113*, 2282.

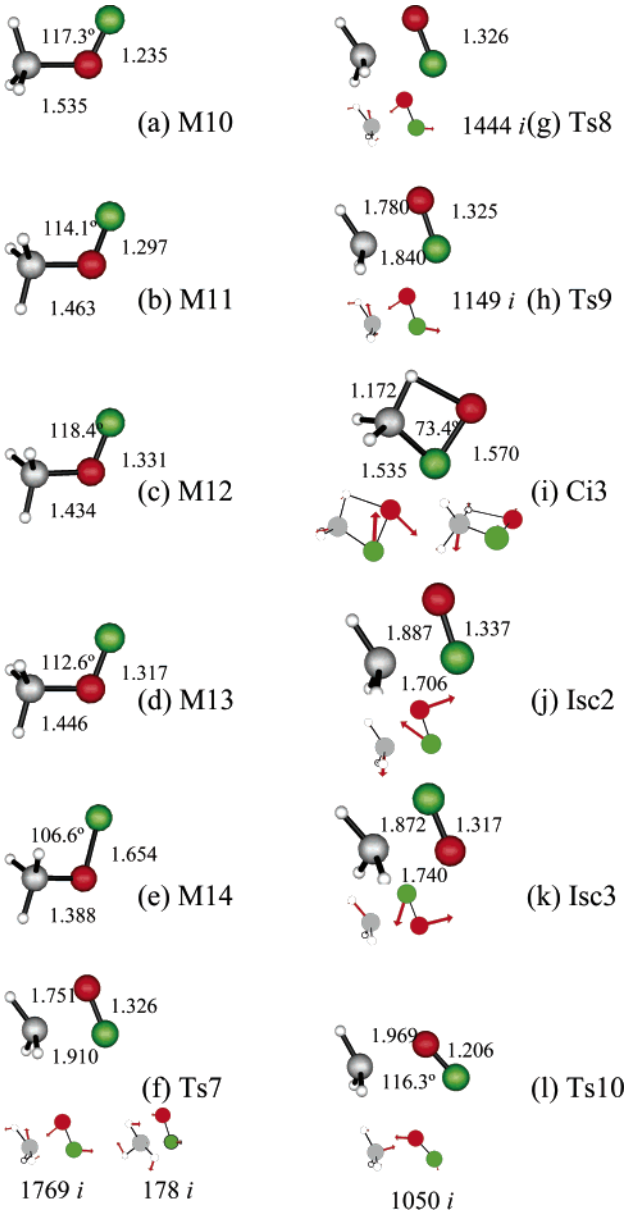

FIGURE 7. CASPT2 geometries for the isomerization of nitrosomethane to methoxy nitrene. The arrows in the smaller structures correspond to the (i) imaginary modes (for stationary points), (ii) nonadiabatic coupling (right) and gradient difference (left) vectors (for conical intersections), or (iii) gradient difference vector (intersystem crossings). (a) S_0 methoxy nitrene (1A′); (b) S_1 methoxy nitrene (1A″); (c) S2 methoxy nitrene (2A′); (d) T_1 methoxy nitrene (1^3A″); (e) T2 methoxy nitrene (1^3A′); (f) S_0 transition state for isomerization (1A′); (g) S_1 transition state for isomerization (1A″); (h) T_1 transition state for isomerization (1^3A″); (i) S_1/S_0 conical intersection; (j) T_1/S_0 intersystem crossing; (k) S_0/T_1 intersystem crossing; (l) T_1 transition state for dissociation or recombination (1^3A″). Structures are represented with the MacMolplt program.[32]

hydroxy nitrene (HON), which may play an important role in combustion and atmospheric chemistry, was recently detected.[30] In this section, we document the main features related to the isomerization reaction of nitrosomethane to methoxy nitrene (CH_3ON). Figure 7 displays the structures found in the domain of the potential energy surfaces (ground and excited states) of

(30) Maier, G.; Reisenauer, P.; De Marco, M. *Angew. Chem., Int. Ed* **1999**, *38*, 108.

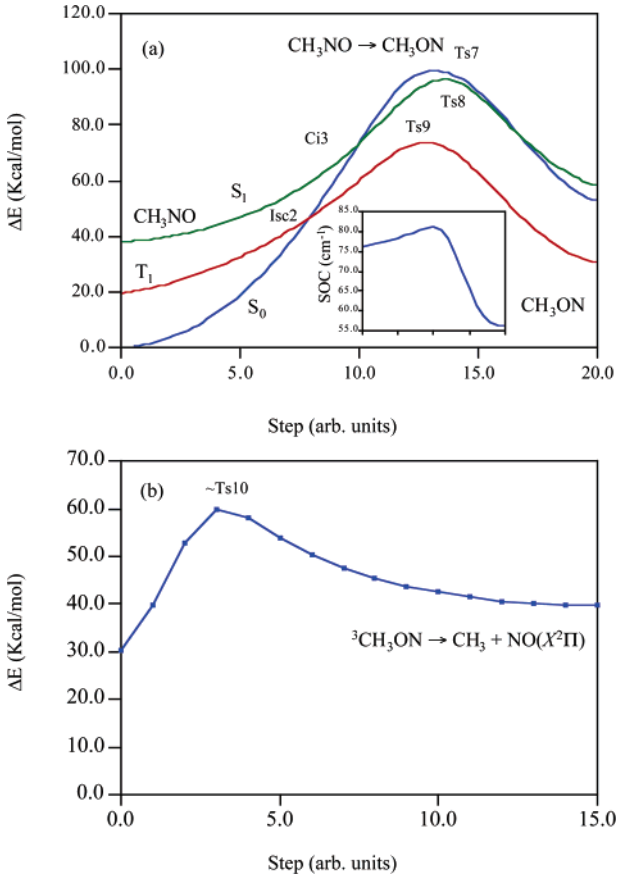

FIGURE 8. (a) CASPT2 linear interpolations for the nitrosomethane to methoxy nitrene isomerization in the S_0, S_1, and T_1 surfaces (CASPT2). Spin−orbit coupling is represented in the inset. (b) CASPT2 linear interpolation for the dissociation of the T_1 ground state of methoxy nitrene.

TABLE 5. CASPT2 Energies of the Critical Points of the Dissociation of Nitrosomethane into Methyl and Nitric Oxide on the Singlet and Triplet Surfaces[a]

geometry	configuration	Δ*E* (kcal/mol)
M1, Figure 1a, 1A′	ground state	0.0
M10, Figure 7a, 1A′	closed shell	51.4
M11, Figure 7b, 1A″	$(n_\sigma)^1(\pi^*_{NO})^1$	57.3
M12, Figure 7c, 2A′	$(n_\sigma)^0(\pi^*_{NO})^2$	98.0
M13, Figure 7d, 1^3A″	$(n_\sigma)^1(\pi^*_{NO})^1$	29.8
M14, Figure 7e, 1^3A′	$(\pi_{NO})^1(\pi^*_{NO})^1$	143.8
Ts7, Figure 7f, 1A′	ground state	109.1
Ts8, Figure 7g, 1 A″	$(n_\sigma)^1(\pi^*_{NO})^1$	97.1
Ts9, Figure 7h, 1^3A″	$(n_\sigma)^1(\pi^*_{NO})^1$	73.5
Ci3, Figure 7i, 1A″/1A′	S_1/S_0	70.6
Isc2, Figure 7j, 1^3A″/1A′	T_1/S_0	46.0
Isc3, Figure 7k, 1A′/1^3A″	S_0/T_1	47.2
Ts10, Figure 7l, 1^3A″	$(n_\sigma)^1(\pi^*_{NO})^1$	51.6

[a] ANO-L basis sets (I) and CAS-SCF (12e, 9o) reference wave function.

methoxy nitrene. Three minima have been localized on the singlet surfaces, S_0 (1A′, M10, Figure 7a), S_1 (1A″, M11, Figure 7b), and S_2 (2A′, M12, Figure 7c). On the triplet surfaces, we found two minima, T_1 (1^3A″, M13, Figure 7d) and T_2 (1^3A′, M14, Figure 7e).

The ground state of methoxy nitrene is a triplet state with a staggered conformation (M13), which is ∼30 kcal/mol above the minimum of nitrosomethane (M1). The energy profiles connecting the S_0, S_1, and T_1 states are represented in Figure 8a, which shows noticeable barriers for the direct isomerization

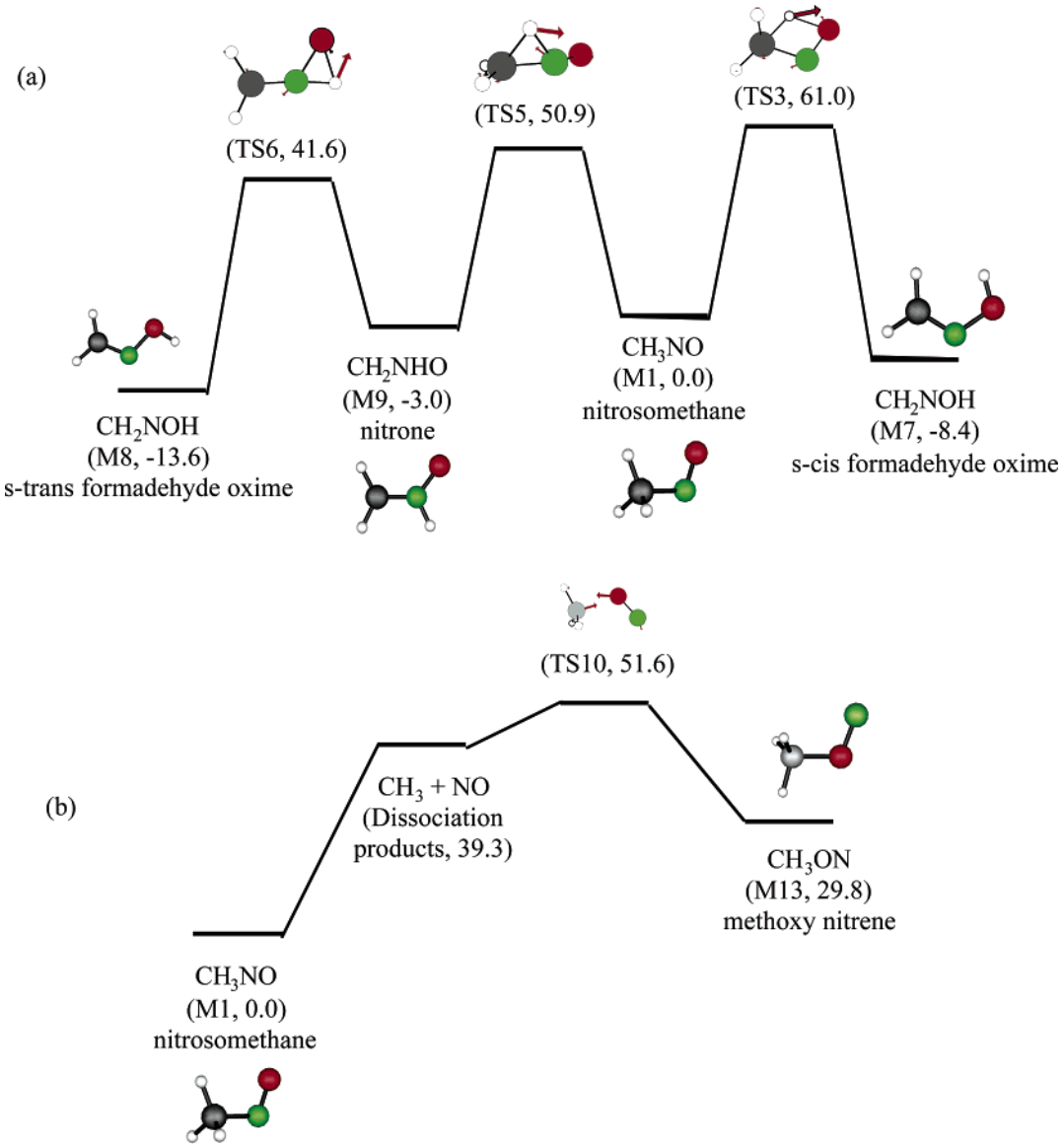

FIGURE 9. Schematic representation of the reaction paths of nitrosomethane in the ground electronic state. (a) Tautomerization reactions of (i) nitrosomethane to *s-cis*-formaldehyde oxime, (ii) nitrosomethane to formyl nitrone, and (iii) formyl nitrone to *s-trans*-formaldehyde oxime. (b) The channel for the dissociation of nitrosomethane followed by the recombination to methoxy nitrene. Relative energies with respect to S_0 nitrosomethane are given in parentheses in kcal/mol.

reactions. The barriers of these paths amount to 57.7 kcal/mol (Ts7, S_0, Figure 7f), 39.8 kcal/mol (Ts8, S_1, Figure 7g), and 43.8 kcal/mol (Ts9, T_1, Figure 7h). Therefore, these values prevent a direct isomerization. As it can be seen in Figure 8a as well, several surface crossings occur along the reaction paths. In fact, we have found one S_1/S_0 conical intersection (Ci3, Figure 7i) and two intersystem crossings, T_1/S_0 (Isc2, Figure 7j) and S_0/T_1 (Isc3, Figure 7k). Isc3 should correspond to a path not included in Figure 8a.

The preceding discussion has discarded the route for direct isomerization. Consequently, we have to admit that the methoxy nitrene has to be formed by the collision of the CH_3 and NO fragments. Figure 8b represents the linear interpolation for the recombination/dissociation channel of CH_3ON; the actual energy barrier for recombination amounts to ~12 kcal/mol (Ts10, T_1, Figure 7l). The approximate sign in front of TS10 in Figure 8b denotes that this point does not correspond to the actual transition state, but it is the starting point for the optimization of such a point. The energies of all the geometries discussed in this section are summarized in Table 5.

Summary

The dissociation reaction of nitrosomethane into methyl and nitric oxide has been studied. In addition, the tautomerization reactions to formaldehyde oxime, nitrone, and methoxy nitrene have been investigated. The prevailing reactions in both the ground and the excited states are dissociations. The energy barriers for the three isomerizations are relatively high in the gas phase; therefore, these reactions are of minor importance in the gas phase. Alternatively, methoxy nitrene could be formed by a bimolecular collision between methyl and nitric oxide. Figure 9 represents schematically the reaction paths described above.

To finish, we can compare the geometries and the energetics of the ground and excited states obtained with the CASPT2 and

CAS-SCF methods, respectively. Tables S1 to S4 (see Supporting Information) illustrate the effect of including the correction for dynamical electron correlation. It is observed in these tables that the differences between the two methods for individual changes in bond lengths are of the order of 0.01−0.02 Å, while the characters and CASPT2 energetics of the CAS-SCF geometries remain similar. These conclusions agree with a recent article that compares structures obtained with these two approaches.[31] In addition, it must be noted that our CASPT2 geometrical parameters compare quite well with the experimental values and with those obtained at the MP2/RHF level.[1]

(31) Page, C. S.; Olivucci, M. *J. Comput. Chem.* **2003**, *24*, 298.
(32) Bode, B. M.; Gordon, M. S. *J. Mol. Graphics Modell.* **1999**, *16*, 133.

Acknowledgment. This research has been supported by the Spanish Ministerio de Educación y Ciencia (Project BQU2003-1426). The authors thank SCAI (University of Málaga) economical support for providing the MOLCAS 6.2 software package. D.P. thanks the Spanish Ministerio de Educación y Ciencia for Grant BES-2004-6033.

Supporting Information Available: Tables of geometrical parameters (CAS-SCF and CASPT2), tables of energetics (CAS-SCF and CASPT2), orbital contour plots of nitrosomethane, and energy profiles of the isomerization reactions. This material is available free of charge via the Internet at http://pubs.acs.org.

JO051897R